

## Copper-Silver Bimetallic Nanoparticles Synthesized by Electrochemical Reduction Method

Sunita Jadhav\*, Nita Dongare

Department of Chemistry, Hutatma Rajguru Mahavidyalaya, Rajgurunagar 410505, Maharashtra, India

### ABSTRACT

Copper-Silver bimetallic nanoparticles were synthesized by electrochemical reduction method which is environmental benign. The tetra butyl ammonium bromide (TBAB) used as stabilizing agent in an organic medium *viz.* tetra hydro furan (THF) and acetonitrile (ACN) in 4:1 ratio by optimizing current density. The parameters such as current density, solvent polarity, distance between electrodes, and concentration of stabilizers are used to control the size of nanoparticles. The synthesized copper-silver bimetallic nanoparticles were characterized by using UV-Visible, FT-IR, XRD, SEM-EDS and TEM analysis techniques.

**Keywords :** Electrochemical cell, Tetra butyl ammonium bromide, Copper-Silver bimetallic nanoparticles, SEM, TEM and XRD.

### I. INTRODUCTION

Bimetallic nanoparticles exhibit interesting electronic, optical, biological and chemical properties due to new bifunctional or synergistic effects [1-11]. As the demand increases for the materials with antimicrobial properties, new methods of obtaining metal nanoparticles are constantly increasing [12]. Silver and copper nanoparticles are used as additives to enhance the biocidal activity of medical materials, textiles, paints and varnishes, plastics and other materials [13]. A combination of the antibacterial properties of silver and the antifungal properties of copper allows the generation of a material with a wide spectrum of action against microorganisms [14,15]. Silver nanoparticles are the most broadly described nanomaterials [16,17], which are highly effective against bacteria and can be found in many commercial products [18]. Nanosilver despite the many advantages such as the low concentrations that

are sufficient to limit bacterial proliferation, a wide range of activities and simple methods to produce stable suspensions, materials are also sought that would work well as a biocide whilst limiting the negative effects of nanosilver [19,20]. Examples of particles with similar effects to Ag are copper nanoparticles (Cu), which also have a high antimicrobial activity, especially antifungal [21]. In addition, Cu is more affordable and more accessible than Ag [22]. The main advantage of using Cu is the obtaining a stable suspension with a concentration of nanoparticles that ensures sufficient biocidal activity. The process of obtaining Cu is time-consuming, and the nanoparticles themselves usually have a larger size compared to Ag, which may decrease the biocidal activity of Cu [23]. In this report, we describe the synthesis and characterization of Cu-Ag bimetallic nanoparticles with tetra butyl ammonium bromide as stabilizing agent.

## II. METHODS AND MATERIAL

### Experimental:

Copper-silver bimetallic nanoparticles were synthesized by electrochemical reduction method. In the initial experiment we have used electrolysis cell to carry out electrolysis process. In this cell, two anodes (Cu and Ag) were positioned in such a way that they lie parallel to each other and apart from each other by a distance of 1x1 cm. The inert cathode, platinum foil was placed between the two anodes and it was perpendicular to both of them. In typical procedure, the above electrolysis vessel having anode (Cu-Ag) 1 x 1cm and a platinum cathode (1 x 1cm) were employed in the preparation of Cu-Ag bimetallic nanoclusters. A mixture of acetonitrile and tetrahydrofuran (4:1) was used as solvent. The supporting electrolyte consisted of solution of ligand, tetra butyl ammonium bromide TBAB at 0.01M. The supporting electrolyte used also act as stabilizer in the formation of bimetallic nanoclusters. Electrolysis was carried out at room temperature by passing the current of various current densities 10 mA/cm<sup>2</sup> for two hours. The colour changes were observed and noted during the electrolysis process. After two hours of electrolysis process the concentration of the nanoparticles increased sufficiently leading to their agglomeration process. After the electrolysis time, the solid particles of the nanoparticles settled at the bottom of the vessel. The reaction mixture was transferred into the clean and dry bottle along with solid particles and then after 15 to 20 minutes decantation process was followed for separation. The solid as well as the supernatant were collected separately. The solid sample was washed 2 to 3 times with THF to remove the excess ligand. The samples were then dried in vacuum desiccator and further stored in airtight capsules for characterization.

### Characterization:

The prepared copper-silver bimetallic nanoparticles were characterized by UV-Visible spectrophotometer, FT-IR spectrophotometer, XRD, TEM, SEM-EDS

techniques. The UV-visible spectra were recorded on UV-Visible spectrophotometer [JASCO 503] using a quartz cuvette with ACN / THF (4:1) as reference solvent. The IR spectra were recorded on FT-IR spectrophotometer [JASCO, FT-IR/4100] Japan using dry KBr as standard reference in the range of 600 – 4000 cm<sup>-1</sup>. The X-ray powder diffraction patterns of the copper oxide nanoparticles were recorded on Bruker 8D advance X-ray diffractometer using CuK $\alpha$  radiation of wavelength = 1.54056 Å. To study the morphology and elemental composition copper (II) oxide nanoparticles were examined using SEM and energy dispersive spectrophotometer (EDS). The SEM analysis was carried out with JEOL; JSM-LA operated at 20.0 kV and 1.0000 nA. Shape, size and morphology were calculated by TEM analysis was using Philips model CM200 operated at 200 kV.

## III. RESULTS AND DISCUSSION

Figure 1 shows the UV-visible spectra of Cu-Ag bimetallic nanoparticles. The surface plasmon resonance is the most remarkable optical property of metal colloids and nanoparticles. The alloy formation is confirmed by the optical absorption spectra that shows two surface plasmon peaks and the position of the  $\lambda_{\max}$  depends upon the composition.

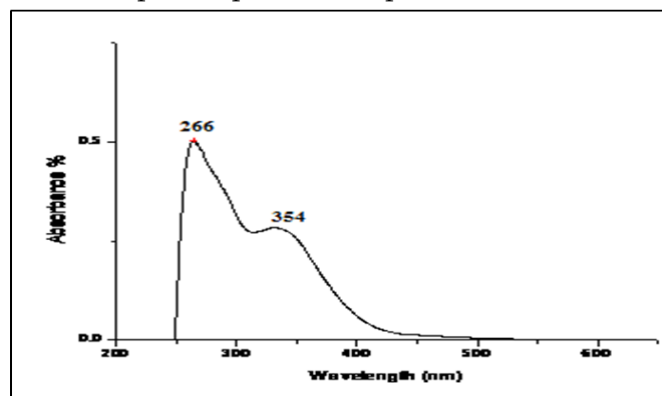


**Figure 1.** UV-visible spectrum of Cu-Ag nanoparticles capped with TBAB

The analysis of the prepared sample of Cu-Ag bimetallic nanoparticles reveals the chemical properties of nanoparticles. On the basis of the FTIR

spectra we have obtained the results for the surface chemistry of the nanoparticles. The frequencies for the different functional groups have been reported [24-26]. The position and the presence of these functional groups can be detected by the FTIR technique. The Fig. 2 shows the IR spectrum of the as prepared sample of Cu-Ag bimetallic nanoparticles capped with TBAB. Peak at  $3736\text{cm}^{-1}$  corresponds to the O-H stretching band. This arises due to the absorption of water molecules by the sample during storage. The broad peak at  $3036\text{cm}^{-1}$  and a narrow peak at  $2879\text{cm}^{-1}$  correspond to the C-H stretching vibrations. The peak at  $1784\text{cm}^{-1}$  corresponds to the  $\text{CO}_2$  which is absorbed by the sample. The peak at  $1684\text{cm}^{-1}$  is related to the symmetrical ammonium ion ( $\text{N}^+\text{R}_4$ ). The frequency at  $1491\text{cm}^{-1}$ ,  $1442\text{cm}^{-1}$  and  $1354\text{cm}^{-1}$  corresponds to the C-H bending vibrations. The C-N linkage in the  $\text{N}^+\text{R}_4$  gives a medium band at  $1236\text{cm}^{-1}$  and  $1134\text{cm}^{-1}$ , which are due to the stretching vibrations. The peak at  $833\text{cm}^{-1}$  and  $690\text{cm}^{-1}$  corresponds to the  $\text{CH}_2$  rocking. These results indicate that the capping agent TEAB has been adsorbed on the surface of the Cu-Ag bimetallic nanoparticles. The spectrum also contains bands at  $401\text{cm}^{-1}$ ,  $453\text{cm}^{-1}$  and  $540\text{cm}^{-1}$  are due to the silver nanoparticles.

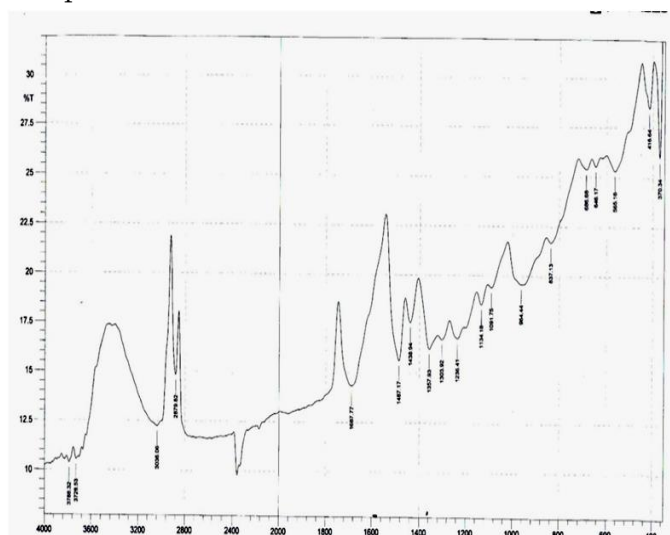


Figure 2 FTIR spectrum of Cu-Ag bimetallic nanoparticles.

The X-ray diffraction pattern of the Cu-Ag bimetallic nanoparticles synthesized with TBAB capping agent at  $10\text{mA}/\text{cm}^{-2}$  is shown in Fig.3 which indicates the crystalline nature of particles. The peaks at  $2\theta$  values of corresponding plane (010), (011), (111), (201), (211), (003), (021) and (312) show the monoclinic structure of copper oxide nanoparticles (ASTM No. 7421).

The peaks at planes (110), (200), (220), (221), (310), (311) and (222) indicate the cubic structure of silver oxide nanoparticles. The data is matched with ASTM card no. 04-0783. The peak at  $76.878^\circ$  is the strongest peak of copper is overlapped with the peak of silver can be assigned (311) plane of the cubic structure of Ag. The mean size of Cu-Ag nanoparticles obtained from the half width of the (011) different peak using the Scherrer equation is about  $8.56\text{nm}$  which accords with the results of TEM image for the particle sizes.

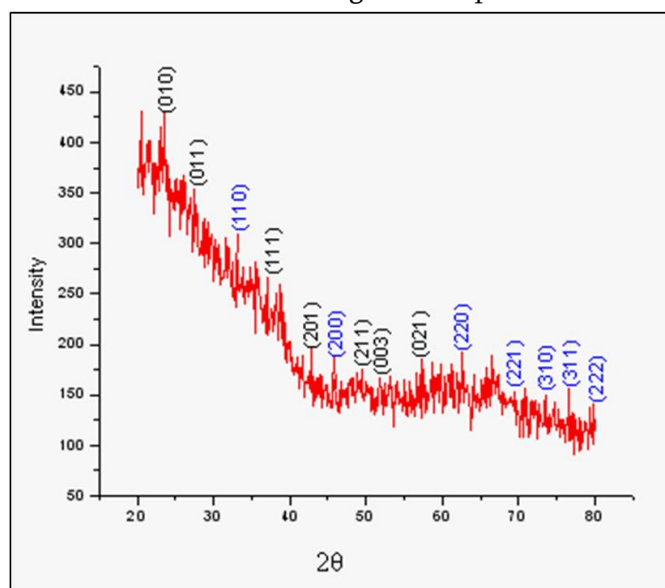


Figure 3 XRD Spectra of Cu-Ag bimetallic nanoparticles

**Table 5.A.5.1.** XRD analysis data for Cu-Ag bimetallic nanoparticles

h	k	l	2 $\theta$ (°) (Exp)	2 $\theta$ (°) (Cal)	d(A°) (Exp)	d(A°) (Cal)	Intensity (Exp)
0	1	0	26.688	26.111	3.33753	3.41000	139.39
0	1	1	31.162	31.520	2.86781	2.83609	141.69
1	1	1	37.839	37.094	2.37571	2.42170	846.83
2	0	1	43.016	42.670	2.10103	2.11724	44.30
2	1	1	51.486	50.713	1.77352	1.79873	178.60
0	0	3	54.402	53.797	1.68513	1.70267	65.82
0	2	1	57.173	56.887	1.60986	1.61728	43.27
3	1	2	76.878	77.133	1.23906	1.23560	37.40
1	1	0	30.924	30.925	2.88936	2.88924	808.36
2	0	0	44.324	44.301	2.04201	2.04300	746.46
2	2	0	64.497	64.447	1.44360	1.44462	253.03
2	2	1	69.701	68.883	1.34800	1.36200	71.00
3	1	0	73.239	73.190	1.29137	1.29211	166.33
3	1	1	77.496	77.402	1.23071	1.23197	188.02

The shape and size distribution of nanostructures were characterized by scanning electron microscopy. Fig.4 A and Fig.4. B illustrates typical morphologies of Cu-Ag bimetallic nanoparticles synthesized with TBAB capping agent with 10mA current density. The result shows they contains many tiny amorphous particles which show the polycrystalline sheet like morphology of Cu-Ag bimetallic nanoparticles. The Fig.4 A shows the microgram at a resolution of 0.5  $\mu\text{m}$  wherein it is seen that the nanoparticles are in clumps and the structure is discontinuous in nature. The resolution at 1.0  $\mu\text{m}$ , in Fig.4 B shows a morphology of the nanoparticles that resembles like agglomerated particles with irregular shape.

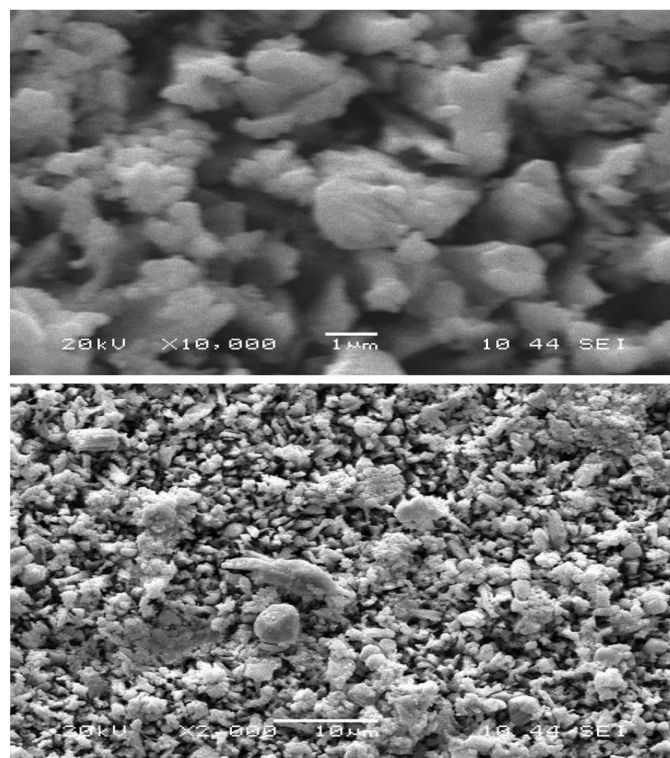
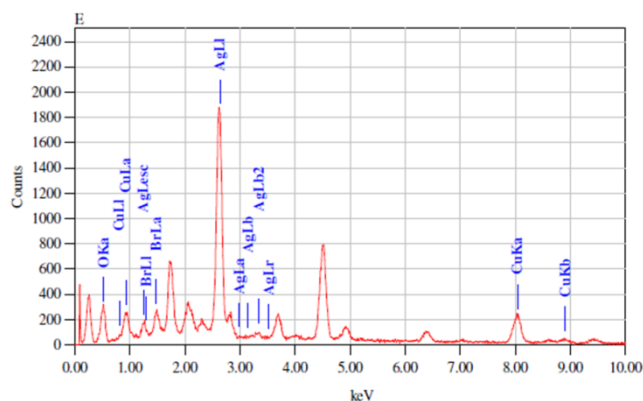


Figure 4 A and 4 B Scanning Electron Microscopic images.

The EDS spectrum of sample (Fig. 5) prepared by using TBAB as capping agent at 10mA current density shows peaks corresponding to Cu, Ag, O and Br. The analysis of spectra gives wt% and atom% of each element present in sample. The content of elements according to their wt% and atom% is shown in Table 5. In this the wt% and atom% of copper and silver clearly shows the formation of Cu-Ag bimetallic nanoparticles.



**Table 5.** EDS analysis of Cu-Ag nanoparticles

Constituent	Mass (%)	Atom (%)
Cu	80.52	69.15
Ag	15.78	13.19
O	7.38	24.45
Br	0.32	0.21

The physical properties of the nanosized materials depend upon the size, morphology and aggregation of the particles. These details can be better understood by a commonly used technique, Transmission Electron Microscopy (TEM). The metal nanoparticles especially those consisting of noble (precious) metal elements, give high contrast [27] when the particles are placed on a thin carbon film supported by metal grids. For large crystalline metal nanoparticles, HRTEM can suggest the area composition by the fringe measurement, giving crystal information of the nanoparticles observed in the particle image [28-30]. In order to characterize the nanoparticles using TEM, a solution containing the prepared Cu-Ag

nanoparticles in ethanol was sonicated for 15 minutes. A single micro drop of this solution was allowed to dry on a carbon coated copper grid for TEM imaging. The nanoparticles exhibit nearly spherical shape and most of them aggregate together even under ultrasonic vibration for a long time. The average size of these nanoparticles is about 1-45nm, almost in accordance with that from SEM and XRD observations.

Fig.6 shows the Cu-Ag bimetallic nanoparticles, these are variable in size and spherical in shape.

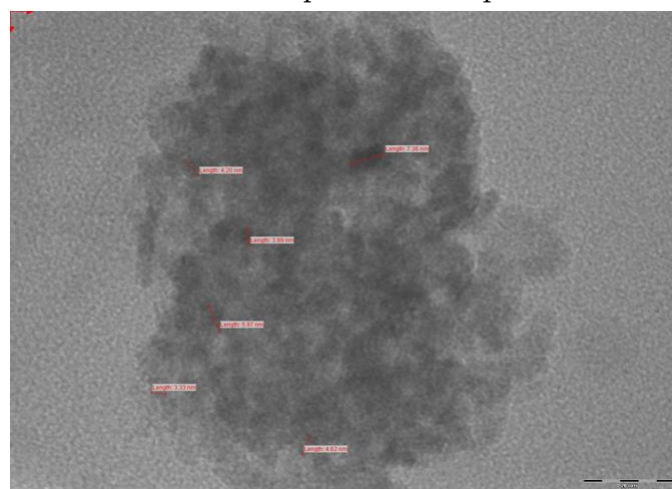


**Figure 6** TEM of Cu-Ag bimetallic nanoparticles capped with 0.01M TEAB at current density 10 mA/cm<sup>2</sup>

#### IV. CONCLUSION

In summary, we have demonstrated the efficiency of electrochemical reduction method for the synthesis of Cu-Ag bimetallic nanoparticles. The TBAB salts used as ligands have played a significant role on controlling the particle size. The procedure offers several advantages including control the particles size, excellent yields, operational simplicity and minimum environmental effects. The copper silver bimetallic nanoparticles had average size in the range of 5 – 30 nm. Thus, the synthesis of Cu-Ag Bimetallic nanoparticles by electrochemical reduction method is easiest, cheapest, require less time and high purity of nanoparticles are obtained.



## V. REFERENCES

- [1]. Daniel, M. C.; Astruc, D. *Chem. Rev.* 2004, 104, 293.
- [2]. Zhong, C. J.; et.al. In *Nanotechnology in Catalysis*; B. Zhou, S., Hermans, G. A., Somorjai, K., Eds.; Academic/Plenum Publishers: New York, 2004, 1, 222.
- [3]. (a Hostetler, M. J.; Zhong, C. J.; Yen, B. K. H.; Anderegg, J.; Gross, S. M.; Evans, N. D.; Porter, M.; Murray, R. W. *J. Am. Chem. Soc.* 1998, 120, 9396. (b Mallin, M. P.; Murphy, C. J. *Nano Lett.* 2002, 2, 1235,
- [4]. Srnova-Sloufova, I.; Vlckova, B.; Bastl, Z.; Hasslett, T. L. *Langmuir* 2004, 20, 3407.
- [5]. Schmid, G.; West, H.; Mehles, H.; Lehnert, A. *Inorg. Chem.* 1997, 36, 891.
- [6]. Shi, H. Z.; Zhang, L. D.; Cai, W. P. *J. Appl. Phys.* 2000, 87, 1572.
- [7]. Shibata, T.; Bunker, B. A.; Zhang, Z.; Meisel, D.; Vardeman, C. F.; Gezelter, J. D. *J. Am. Chem. Soc.* 2002, 124, 11989.
- [8]. Moskovits, M.; Srnova-Sloufova, I.; Vlckova, B. *J. Chem. Phys.* 2002, 116, 10435.
- [9]. Zhong, C. J.; Maye, M. M. *Adv. Mater.* 2001, 13, 1507.
- [10]. Bradley, J. S. In *Clusters and Colloids*; Schmid, G., Ed.; WileyVCH: Weinheim 1994; Chapter 6.
- [11]. (a Davis, R. J.; Boudart, M. *J. Phys. Chem.* 1994, 98, 5471. (b Via, G. H.; Drake, K. F., Jr.; Meitzner, G.; Lytle, F. W.; Sinfelt, J. H. *Catal. Lett.* 1990, 5, 234.
- [12]. V.K. Sharma, C.M. Sayes, B. Guo, S. Pillai, J.G. Parsons, C. Wang, B. Yan, X. Ma, Interactions between silver nanoparticles and other metal nanoparticles under environmentally relevant conditions: A review, *Sci. Total Environ.* 2019, 653, 1042.
- [13]. W.J. Stark, P.R. Stoessel, W. Wohlleben, A. Hafner, Industrial applications of nanoparticles, *Chem. Soc. Rev.* 2015, 44, 5793.
- [14]. A. Kalińska, S. Jaworski, M. Wierzbicki, M. Gołębiewski, *Int. J. Mol. Sci.* 2019, 20, 1672.
- [15]. T.A.J. Souza, L.P. Franchi, L.R. Rosa, M.A.M.S. da Veiga, C.S. Takahashi, *Mutat. Res. - Genet. Toxicol. Environ. Mutagen.* 2016, 795, 70.
- [16]. M. Rai, A.P. Ingle, S. Birla, A. Yadav, C.A. Dos Santos, *Crit. Rev. Microbiol.* 2015, 42, 696.
- [17]. J. Peszke, M. Dulski, A. Nowak, K. Balin, M. Zubko, S. Sułowicz, B. Nowak, Z. Piotrowska-Seget, E. Talik, M. Wojtyniak, A. Mrozek-Wilczkiewicz, K. Malarz, J. Szade, *RSC Adv.* 2017, 7, 28092.
- [18]. A.K. Biswal, P.K. Misra, *Mater. Chem. Phys.* 2020, 250, 123014.
- [19]. X.-F. Zhang, Z.-G. Liu, W. Shen, S. Gurunathan, *Int. J. Mol. Sci.* 2016, 17, 1534.
- [20]. S. Ahmed, M. Ahmad, B.L. Swami, S. Ikram, *J. Adv. Res.* 2016, 7, 17.
- [21]. A.K. Chatterjee, R. Chakraborty, T. Basu, *Nanotechnology.* 2014, 25, 135101.
- [22]. M.A. Asghar, E. Zahir, S.M. Shahid, M.N. Khan, M.A. Asghar, J. Iqbal, G. Walker, *LWT.* 2018, 90, 98.
- [23]. K.S. Tan, K.Y. Cheong, *J. Nanoparticle Res.* 2013, 15.
- [24]. Sherman, C. P. *Infrared Spectroscopy in, Handbook of Instrumental Techniques for Analytical Chemistry*, F. Settle (Ed.), Prentice Hall Inc., New Jersey.
- [25]. Nakamoto, K. *Infrared Spectra of Inorganic and Coordination Compounds*. John Wiley and Sons, 1963.
- [26]. Pavia, D. L.; Lapman, G. M.; Kriz, G. S. *Introduction to Spectroscopy*, III Edn., Brooks / Cole Cengage Learning, Singapore, 2008.
- [27]. Toshima, N.; Yonezawa, T. *New J. Chem.* 1998, 1179.
- [28]. Schmid, G.; Morun, B.; Malm, J. O. *Angew Chem. Int. Ed. Engl.* 1998, 28, 778.

- [29]. Duff, D. G.; Curtis, A. C.; Edwards, P. P.; Jefferson, D.A.; Logen, D. E. J. Chem. Soc. Chem. Commun. 1987, 1264.
- [30]. Curtis, A. C.; Edwards, P. P.; Duff, D. G.; Jefferson, D. A.; Johnson, B. F. G.; Kirkland, A. I. J. Phys. Chem. 1988, 92, 2270.